ACADEMIA ROMÂNĂ
Revue Roumaine de Chimie
http://web.icf.ro/rrch/

Rev. Roum. Chim.,
2014, *59*(9), 761-767

QUANTUM CHEMICAL INVESTIGATIONS ON PHENYL-7,8-DIHYDRO- [1,3] -DIOXOLO [4,5-*G*] QUINOLIN-6(5*H*)-ONE

Masoome SHEIKHI[a,*] and Davood SHEIKH[b,*]

[a] Young Researchers and Elite Club, Gorgan Branch, Islamic Azad University, Gorgan, Iran
[b] Young Researchers and Elite Club, Hamedan Branch, Islamic Azad University, Hamedan, Iran

Received June 18, 2014

The density functional theory (DFT) calculations was carried out on Phenyl-7,8-dihydro- [1,3] -dioxolo [4,5-*g*] quinolin-6(5*H*)-one with B3LYP method and 6-31G* basis set in gas phase using Gaussian 03. The ^{1}H and ^{13}C NMR chemical shifts, thermodynamic properties, frontier molecular orbital (FMO) analysis, the molecular electrostatic potential (MEP), NBO analysis and total density of states (DOS) of the compound were investigated by theoretical calculations. E_{HOMO}, E_{LUMO} and HOMO-LUMO energy gap (Eg; Δ), Ionisation Potential (I), Electron affinity (A), chemical hardness (η), electronic chemical potential (μ) and electrophilicity (ω) obtained.

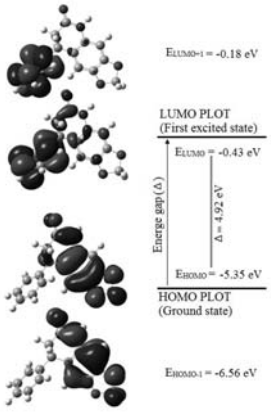

INTRODUCTION

Quinoline derivatives are in a class of biologically active compounds. Quinolines have biological properties such as drug analgesics,[1,2] antiamoebic,[3,4] tryphocidal,[5] antiseptic[6] and antiserotonin.[7] In addition to these, derivatives also exhibit good antimalarial,[8] antitubercular,[9] antibacterial,[10] antihistaminic,[11] antineurodegerative,[12] anticonvulsant,[13] antitumor,[14] anticancer[15] and antiallergics[16] activities. Because of their wide range of biological, industrial and synthetic applications quinolines have recently received a great deal of attention. Because the substituted quinolines have of biological, industrial and synthetic applications, resulting synthesize many new derivatives. Phenyl-7,8-dihydro- [1,3] -dioxolo [4,5-*g*] quinolin-6(5*H*)-one (Fig. 1) is derivative of quinoline which synthesis of using ultrasound-promoted three component one-pot procedure under catalyst-free and solvent-free conditions.[17]

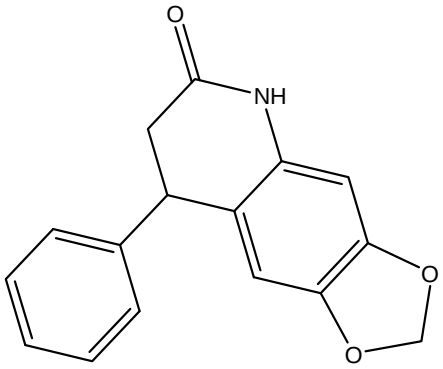

Fig. 1 – Structure
of Phenyl-7,8-dihydro- [1,3] -dioxolo [4,5-*g*] quinolin-6(5*H*)-one.

* Corresponding authors: m.sheikhi@gorganiau.ac.ir and davood.sheikh@iauh.ac.ir

In this work, DFT calculations performed with B3LYP hybrid functional employing the 6-31G* basis sets for Phenyl-7,8-dihydro- [1,3] -dioxolo [4,5-*g*] quinolin-6(5*H*)-one. In addition, HOMO, LUMO and NBO analyses have been used to elucidate the charge transfer within the molecules. The electronic chemical potential (μ), global hardness (η) and electrophilicity index (ω)[18] were calculated.

Computational details

We carried out quantum theoretical calculations of title compound using DFT method (B3LYP) with 6-31G* basis set by the Gaussian 03 program.[19] The ^{1}H and ^{13}C NMR chemical shifts of compound calculated within GIAO approach. Also thermodynamic parameters of compound was studied using B3LYP/6-31G* level and obtained the energy (ΔE), enthalpy (ΔH), Gibbs free energy (ΔG), entropy (S) and constant volume molar heat capacity (C_v).20 Some electronic properties such as energy of the highest occupied molecular orbital (E_{HOMO}), energy of the lowest unoccupied molecular orbital (E_{LUMO}), HOMO-LUMO energy gap (E_g), atomic charges, dipole moment (μ) and Point group were determined. The optimized molecular structure (Fig. 2), HOMO and LUMO surfaces were visualized using GaussView 03 program.[21] We also studied electronic structures using Natural Bond Orbital (NBO) analysis.[22]

Discussion

In the present work, we have calculated the ^{1}H and ^{13}C NMR chemical shifts of molecule using B3LYP/6-31G* level within GIAO approach. The observed ^{1}H and ^{13}C NMR chemical shifts and the calculated amounts of selected groups are given in Table 1. There is an excellent agreement between the experimental and theoretical results.

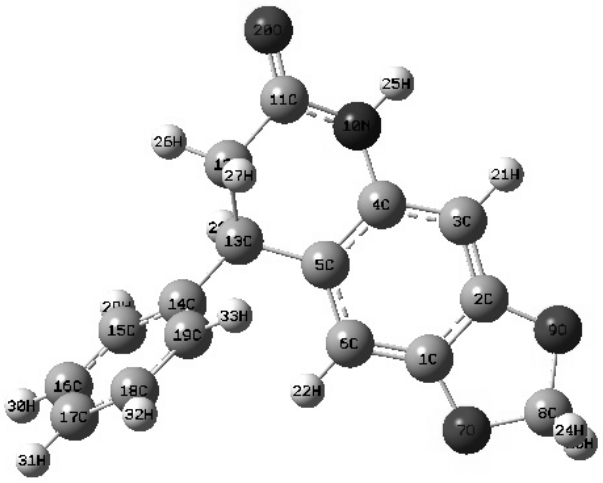

Fig. 2 – Theoretical geometric structure of compound.

Table 1

Experimentally measured and calculated ^{1}H and ^{13}C Chemical Shifts δ (ppm, vs TMS) of title compound

^{1}H-NMR			^{13}C-NMR		
H atom	Cal	Exp[a]	C atom	Cal	Exp[a]
OCH_2	5.55	5.19	OCH_2	92.55	97.7
CH-Ar	4.29-3.57	4.30-4.27	C=O	166.3	168.1
CH_2-C=O	2.99-2.67	3.15-3.08	CH_2-C=O	33.18	39.7
1H Aromatic	6.30	6.33			
5H Aromatic	7.79-7.69	7.41-7.21			

[a] Taken from Ref. [17].

Frequency calculations

The relative energy (ΔE), standard enthalpy (ΔH), entropy (S), Gibbs free energy (ΔG) and constant volume molar heat capacity (C_v) values of title compound obtained by theoretical methods using B3LYP/6-31G* level. The calculated results in Table 2 showed that relative energy, Gibbs free energy and standard enthalpies values is negative values, there for title compound is stable.

As seen in Fig. 3, the atomic charge distribution is different. The N_{10}, O_9, O_7 and O_{20} have more negative charge (-0.720e, -0.536e, -0.534e and -0.502e), respectively. The carbon atoms attached with hydrogen atoms is negative, except C_8 in the five-member ring ($-CH_2$) whereas all the hydrogen atoms carry positive charge. Carbon of carbonyl group (C_{11}) has more positive charge (0.593e) and of hydrogen atoms, H_{25} (-NH) has more positive charge (0.331e). These data clearly show that C_{11} and H_{25} are the two most reactive atoms.

Molecular electrostatic potential

Molecular electrostatic potential (MEP) plots of molecule using B3LYP/6-31G* level was studied. As shown by the MEP maps in Fig. 4, the O_{20} atom (Carbon of carbonyl group) and carbon atoms of phenyl ring are relatively negatively charged (red colors) and lowest electron density, positively charged, is observed for the H_{25} atom (-NH) (blue colors).

Table 2

The calculated thermodynamic parameters of title compound using B3LYP/6-31G* level

ΔE (kcal/mol)	ΔH (kcal/mol)	ΔG (kcal/mol)	S (cal/molk)	CV (cal/molk)
-563302.677	-563302.085	-563339.955	127.020	61.319

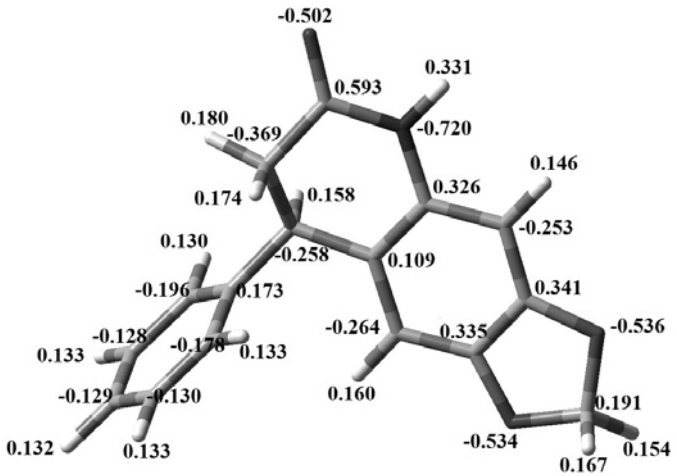

Fig. 3 – Mulliken atomic charge of the atoms of compound.

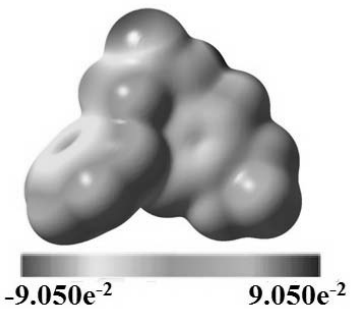

Fig. 4 – The molecular electrostatic potential (MEP) surface of compound.

Natural bond orbital analysis is important method for studying intra- and inter-molecular bonding and interaction between bonds. The results of Natural Bond Orbital (NBO) analysis listed in Table 3 that demonstrate polarization coefficient values of atoms of molecule. According to Table 5, for the C_1-O_7 bond, BD= 0.5730 $sp^{3.12}d^{0.01}$ + 0.8196 $sp^{2.23}d^{0.01}$ reported. Polarization coefficients of C_1= 0.5730 and O_7= 0.8196 reported that show share of contribute O_7 atom in C_1-O_7 bond is greater than share of C_1 atom. In the C_{11}-C_{12} bond BD= 0.6952 $sp^{1.37}$ + 0.7188 $sp^{2.93}$ reported. As seen polarization coefficient values of C_{12} atom (0.7188) is greater than C_{11} atom. The calculated Mulliken charge of C_{12} is negative (-0.369e) whereas C_{11} has positive value (0.593e). In all bonds of C-O, polarization coefficient value of oxygen atom is greater than C atom (see Table 3).

Some electron donor orbital, acceptor orbital and the interacting stabilization energy resulting from the second-order micro disturbance theory are reported. The result of interaction is a loss of occupancy from the concentration of electron NBO of the idealized Lewis structure into an empty non-Lewis orbital. For each donor (*i*) and acceptor (*j*), the stabilization energy *E*(2) associated with the delocalization $i \rightarrow j$ is estimated. The resonance energy ($E^{(2)}$) shows amount of participation of electrons in the resonance. According to results of the NBO analysis (Table 4), the greatest resonance energy ($E^{(2)}$) is 55.37 that LP(1)N_{10} participates as donor and anti-bonding BD*(2)(C_{11}-O_{20}) as acceptor that shows charge is transferred from N_{10} to C_{11}-O_{20} ($N_{10} \rightarrow C_{11}$-$O_{20}$). The calculated Mulliken charges of N_{10} (-0.720e) and C_{11} (0.593e) that taking part in intramolecular charge transfer is indicates in the NBO analysis. Also BD(2)(C_{14}-C_{15}) participates as donor and the anti-bonding BD*(2)(C_{16}–C_{17}) and BD*(2)(C_{18}–C_{19}) interactions as acceptor, respectively. The resonance energy ($E^{(2)}$) in transfer of electron density from BD(2)(C_{14}-C_{15}) of phenyl ring to the anti-bonding BD*(2)(C_{16}–C_{17}) and BD*(2)(C_{18}–C_{19}) of phenyl ring is 20.53 and 19.25, respectively. This indicates the more charge transfer from BD(2)C_{14}-C_{15} to anti-bonding acceptor BD*(2)C_{16}-C_{17}.

Table 3

Calculated natural bond orbitals (NBO) and the polarization coefficient for each hybrid in bonds of compound

A-B	A	B
C_1-C_2	$sp^{1.90}$ (0.7056)	$sp^{1.87}$ (0.7086)
C_1-O_7	$sp^{3.12}d^{0.01}$ (0.5730)	$sp^{2.23}d^{0.01}$ (0.8196)
C_1-C_6	sp (0.7121)	sp (0.7021)
C_2-C_3	$sp^{3.64}d^{0.01}$ (0.5637)	$sp^{2.90}d^{0.01}$ (0.8260)
C_2-O_9	$sp^{3.11}d^{0.01}$ (0.5735)	$sp^{2.19}d^{0.01}$ (0.8192)
C_4-C_5	sp (0.6958)	sp (0.7182)
C_4-N_{10}	$sp^{2.71}$ (0.6232)	$sp^{1.73}$ (0.7821)
O_7-C_8	$sp^{2.87}d^{0.01}$ (0.8245)	$sp^{3.57}d^{0.01}$ (0.5659)
C_8-O_9	$sp^{3.64}d^{0.01}$ (0.5637)	$sp^{2.90}d^{0.01}$ (0.8260)
N_{10}-H_{25}	$sp^{2.73}$ (0.8487)	s (0.5288)
C_{11}-C_{12}	$sp^{1.37}$ (0.6952)	$sp^{2.93}$ (0.7188)
C_{11}-O_{20}	$Sp^{2.05}$ (0.5901)	$Sp^{1.42}d^{0.01}$ (0.8073)

Table 4

Second order perturbation theory analysis of Fock matrix in NBO basis threshold for compound

Donor NBO (i)	Acceptor NBO (j)	$E^{(2)}$
BD(1)C_1-C_6	BD*(2)(C_2-C_3)	21.75
BD (2)C_1-C_6	BD*(2)(C_4-C_5)	17.33
BD(2)C_{14}-C_{15}	BD*(2)(C_{16}-C_{17})	20.53
BD(2)C_{14}-C_{15}	BD*(2)(C_{18}-C_{19})	19.25
BD(2)C_{16}-C_{17}	BD*(2)(C_{14}-C_{15})	19.86
BD(2)C_{16}-C_{17}	BD*(2)(C_{18}-C_{19})	20.45
BD(2)C_{18}-C_{19}	BD*(2)(C_{14}-C_{15})	20.37
BD(2)C_{18}-C_{19}	BD*(2)(C_{16}-C_{17})	19.66
LP(2)O_7	BD*(2)(C_1-C_6)	25.50
LP(2)O_9	BD*(2)(C_2-C_3)	28.21
LP(1)N_{10}	BD* (2)(C_4-C_5)	33.33
LP(1)N_{10}	BD * (2)(C_{11}-O_{20})	55.37
LP(2)O_{20}	BD * (1)(N_{10}-C_{11})	26.77
LP(2)O_{20}	BD * (1)(C_{11}-C_{12})	20.30

Electronic properties

Quantum chemical methods are important for obtain information about molecular structure and electrochemical behavior. In this work, theoretical calculations were employed by DFT method using B3LYP level and 6-31G* basis set. According to Fig. 5, we found charge transfer taking place within the molecule. The HOMO and HOMO-1 orbitals were localized mainly on the fused tricyclic of the molecule whereas LUMO and LUMO+1orbitals were localized mainly on the phenyl ring. The calculated values are -6.56, -0.5.35, -0.43 and -0.18 eV for E_{HOMO-1}, E_{HOMO}, $E_{LUMO,}$ E_{LUMO+1} and HOMO–LUMO gap (ΔE), respectively. The energy of the HOMO is directly related to the ionization potential and the energy of the LUMO is directly related to the electron affinity. The HOMO–LUMO gap (ΔE), is 4.92 eV that large energy gap implies high stability for the molecule.[23-25]

Ionisation Potential (I), Electron affinity (A), chemical hardness (η), electronic chemical potential (μ) and electrophilicity (ω) of molecule were calculated listed in Table 5.

DOS (Total electronic densities of state) analysis indicates E_{HOMO}, E_{LUMO} and HOMO-LUMO energy gap (E_g) molecules. As seen in Fig. 5, E_g of compound is 4.92 eV that obtained using B3LYP/6-31G* level.

CONCLUSIONS

In the present work, we have performed theoretical analyses of Phenyl-7,8-dihydro- [1,3] - dioxolo [4,5-*g*] quinolin-6(5*H*)-one and electronic properties and geometric parameters have been analyzed by DFT/B3LYP calculations. The ^{1}H and ^{13}C NMR chemical shifts of molecule have calculated and determined the experimental data showed have been found to support each other. According to the thermodynamic parameters, we found this structure is stable. MEP analysis shows the maximum electron density is located on the O_{20} atom and carbon atoms of phenyl ring. According to results of the NBO analysis, the greatest resonance energy ($E^{(2)}$) is obtained for LP(1)N_{10} that participates as donor and anti-bonding

BD*(2)(C_{11}-O_{20}) as acceptor that shows charge is transferred from N_{10} to C_{11}-O_{20} (N_{10}→C_{11}-O_{20}). As shown FMO analysis, charge transfer taking place within the molecule and the HOMO is focused mainly on the fused tricyclic and LUMO on the phenyl ring. The HOMO-LUMO energy gap (E_g) molecule was measured 4.92 eV.

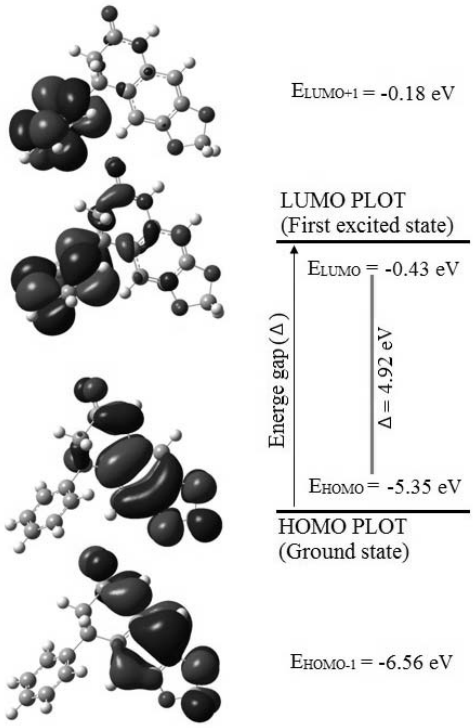

Fig. 5 – Frontier molecular orbitals of compound (Δ: Energy gap between LUMO and HOMO).

Table 5

HOMO, LUMO, energy gaps (HOMO –LUMO) and related molecular properties of title compound (eV)

Energy(Hatree-Fock)	-897.956
μ_D /Debye	3.49
E_{HOMO} /eV	-5.35
E_{LUMO} /eV	-0.43
E_{HOMO-1} /eV	-6.56
E_{LUMO+1} /eV	-0.18
Energy gap (E_g) /eV	4.92
Ionisation Potential (I= - E_{HOMO}) /eV	5.35
Electron affinity (A= - E_{LUMO}) /eV	0.43
Chemical potential (μ=-(I + A)/2) /eV	-2.89
Global Hardness (η = (I – A)/2) /eV	2.46
Global Electrophilicity ($\omega = \mu^2/2\eta$) /eV	1.70

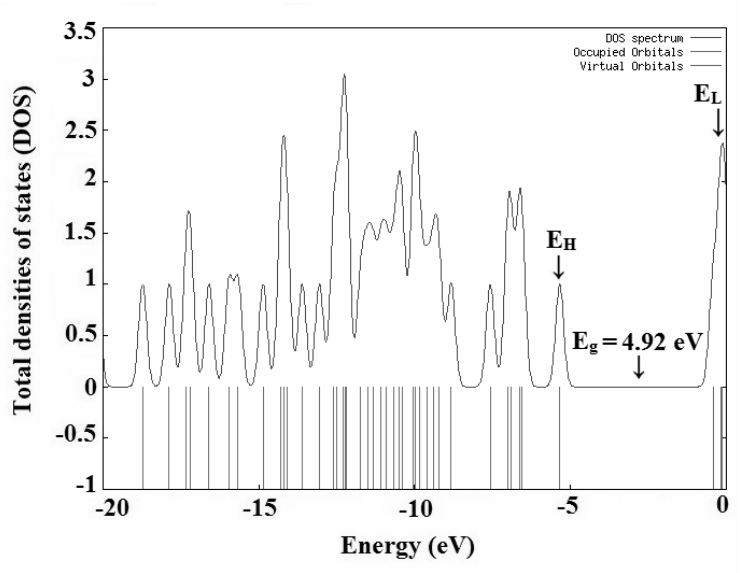

Fig. 6 – Total densities of states (DOS) for compound.

REFERENCES

1. J. Wiesner, R. Ortmann, H. Jomaa and M. Schlitzer, *Angew. Chem .Int.Ed.*, **2003**, *43*, 5274-5293.
2. R. Sevim and K. Guniz, *Molecules*, **2007**, *12*, 1910-1939.
3. A.S. Haythem, M.M. Ibrahim and S.M. MohammaD, *Molecules*, **2009**, *14*, 1483-1494.
4. S.S. Chakravarti, P.K. Sen, S. Choudhari and M. Das, *Ind. J. Chem.*, **1985**, *248*, 737.
5. C.H. Browning, *Proc. R. Soc. London*, **1932**, 372.
6. C.H. Browning, *J. Path. Bact.*, **1924**, *27*, 121-122.
7. M.K. Barbara, B.B. Gordan, D. Michel and H.R. Karl, *Antimicrobial Agents and Chemotharpy*, **1997**, *41*, 1369-1374.
8. L.A. Freek, J.L. Martin and W. Rowlett, *J. Am. Chem. Soc.*, **1946**, *68*, 1285.
9. I.V. Ukrainets, L. Yangyang, A.A. Tkach and A.V. Turov, *Chemistry of Heterocyclic Compounds*, **2009**, *45*, 802-808.
10. M.F. El-Z, A.N. Ahmed, A.O. Farghaly and M.A. bd-Alla, *J. Chem. Technol. and Biotechnol.*, **1992**, *53*, 329 336.
11. C.H. Lee and H.S. Lee, *J. Korean Soc. Appl. Biol.Chem*., **2011**, *54*, 118-123.
12. Z. Hailin, L. Weiner, O. Bar-Am, E. Silvina, Z. Ioav Cabantchik, A. Warshawsky, B.H. Youdimb and M. Fridkina, *Bio. & Med Chemistry*, **2005**, *13*, 773 783.
13. R. Michael, S. Ian, L. Paul, S. Graeme, M. Angela, R. Lesley B. Raymond and A. John, *J. Med. Chem.*, **1993**, *36*, 3386-96.
14. M.P. Wentland, S.C. Aldous, M.D. Gruett, M. R.B. Perni, R.G. Powles, D.W. Danz, K.M. Kingbeil, A.D. Peverly, R.G. Robinson, J.H. Corbett, J.B. Rake and S.A. Coughlin, *Bioorganic and Medicinal Chem. Letters*, **1995**, *5*, 405-410.
15. S.A. Bol, J. Horibeck, J. Markovic, J.G. Boer and R.J. Turesky, *Constable. Carcinogenesis*, **2000**, *21*, 1-6.
16. M.S. Pingle, S.P. Vartale, V.N. Bhosale and S.V. Kuberkar, *Arkivoc*, **2006**, *10*, 190-198.
17. D. Azarifar and D. Sheikh, *Acta Chim. Slov.*, **2012**, *59*, 664-669.
18. K.K. Hazarika, N.C. Baruah and R.C. Deka, *Struct. Chem.*, **2009**, *20*, 1079.
19. M.J. Frisch et al., Gaussian 03, revision B03, Gaussian Inc., Pittsburgh, PA, **2003**.
20. L. Shiri, D. Sheikh, A.R. Faraji, M. Sheikhi and S.A. Seyed Katouli, *Lett. Org. Chem.*, **2014**, *11*, 18-28.
21. A. Frisch, A. B. Nielson and A. J. Holder, GAUSSVIEW User Manual, Gaussian Inc., Pittsburgh, PA, **2000**.
22. M. Sheikhi, D. Sheikh and A. Ramazani, *S. Afr. J. Chem.*, **2014**, *67*, 151-159.
23. D. Habibi, A. R. Faraji, D. Sheikh, M. Sheikhi and S. Abedi, *RSC Adv.*, **2014**, *4*, 47625-47636.
24. P. Politzer and D. G. Truhlar, "Chemical Applications of Atomic and Molecular Electrostatic Potentials", Plenum Press, New York, 1981.
25. P. K. Chattaraj, U. Sarkar and D. R. Roy, *Chem. Rev.*, **2006**, *106*, 2065-2091.